THICK CERAMIC TILES: MICROSTRUCTURAL CHARACTERISTICS AND MECHANICAL BEHAVIOUR

Elisa Rambaldi [1], Luca Magni [2], Cristina Siligardi [2]

[1] ITALCER Group, Italy
[2] Department of Engineering "Enzo Ferrari", University of Modena and Reggio Emilia, Italy

ABSTRACT

In the last year, the substitution of Ukrainian clay by other clays has shown a loss of technical performance in the experimental test mixes at laboratory scale and, in particular, a general low resistance to impact test has been observed especially in thick ceramic tiles (thicker than 20 mm). In the present investigation, the role played by different fluxing raw materials in the densification and crystallisation behaviour during firing was considered. The crystalline index was considered and correlated to the mechanical properties (fracture toughness, elastic modulus and flexural strength). The possibility of reinforcing a standard body mix for porcelain stoneware tiles, by the addition of alumina powders was investigated. The results obtained show that the increase in crack resistance can be attributed to the increase in the crystalline index and, in particular to the presence of alumina particles, since the fracture toughness of these particles is higher than that of the glassy matrix.

1. INTRODUCTION

Thick ceramic tiles, thicker than 20 mm, are produced from traditional porcelain stoneware mixtures. Their ease of installation allows them to be used outdoors, even on uneven surfaces.

As a result of the Russia-Ukraine conflict, the logistical conditions for the supply of raw materials changed and, in particular, an important constituent of porcelain stoneware, Ukrainian clay, was missing. This clay is particularly suitable for contributing plasticity to the unfired body and dimensional stability to the sintered tile. Its replacement by other clays has been difficult, at least initially, resulting in a loss of technical performance in the experimental test mixes.

At laboratory scale, the experimental work was aimed at designing a new mix that was plastic in the unfired state and stable during the firing cycle. Subsequently, the behaviour with thick tiles was evaluated. In some mixes, an increase in a phenomenon sometimes improperly called 'black heart' (otherwise known as 'black core') was observed in thick samples after firing, and a general low resistance to the impact test "CSTB choc répété" (CSTB CAHIER 3778_V4 Annex 11) was also observed.

The aim of this work is to improve the fracture toughness of porcelain stoneware materials. In general, the reinforcing mechanisms are based on control of flaws and toughening [1]. While the first approach concerns control of the critical flaws, by analysing the process and identifying their source, the second approach, acting on the microstructural features, seeks to achieve materials characterised by high reliability and enhanced fracture resistance. The control of critical flaws does not seem to be a viable method, in these materials. Regarding the second approach, there are several ways of modifying the microstructure and toughening a ceramic matrix: (i) toughening transformation, (ii) in situ crystallisation of elongated second phases, (iii) addition of high strength ceramic particles, metal particles and short and long fibres and, (iv) direct metal oxidation.

In the present investigation, the role played by different fluxing raw materials (sodium feldspar, potassium feldspar) in the densification and crystallisation behaviour during firing was studied. The crystalline index was considered and correlated to the mechanical properties (fracture toughness, elastic modulus and flexural strength). In addition, the possibility of reinforcing a standard body mix for porcelain stoneware tiles, by the addition of alumina powders was investigated.

2. MATERIALS AND METHODS

A soda-lime waste glass - from separate urban collection and not suitable for recovery in the glass industry - was added at 5-10-15 wt% in a mix with a traditional sodium feldspar (W0), to develop three new fluxes (W5, W10, W15, respectively).

The chemical composition of the waste glass, the sodium feldspar and the new fluxes, is reported in Tab. I. It was determined by X-ray fluorescence (XRF).

The mineralogical composition of the waste glass is reported in Tab. II. It was determined by X-ray diffraction (XRD), and the Rietveld refinement method with software GSAS was used for quantitative analyses. In Tab. III, the particle size distribution is shown in terms of percentiles.

From a chemical point of view, with respect to the sodium feldspar W0 (without waste glass), the new fluxes are characterized by lower alumina and higher fluxing oxides (CaO, MgO, Na_2O). The amount of organic carbon (C) also increases significantly due to the impurities contained in the waste glass.

	SiO_2	Al_2O_3	TiO_2	Fe_2O_3	CaO	MgO	Na_2O	K_2O	LOI	C	S
Waste glass	72.8	1.5	0.1	0.3	9.2	3.4	11.8	0.7	0.0	0.62	0.01
W0	70.1	17.8	0.1	0.3	1.3	0.2	9.0	0.6	0.6	0.05	0.01
W5	70.2	17.0	0.1	0.3	1.7	0.3	9.1	0.6	0.6	0.8	0.01
W10	70.3	16.2	0.1	0.3	201	0.5	9.3	0.7	0.5	0.10	0.01
W15	70.5	15.4	0.1	0.3	2.5	0.7	9.5	0.7	0.5	0.14	0.01

Table I *– Chemical composition of waste glass, sodium feldspar and new fluxes (wt%).*

	Quartz	Amorphous phase
wt%	2	98

Table II *– Mineralogical composition of the waste glass (wt%).*

	d(10)	d(50)	d(90)
μm	5.04	23.73	66.23

Table III – *Particle size distribution of the waste glass in terms of percentiles (d).*

Ceramic mixes were prepared by substituting the traditional sodium feldspar by the new fluxes (W5, W10, W15), as shown in Tab. IV.

The ceramic mixes contain 40 wt% clays, 10% kaolinitic sand and 50% fluxes: W0 (a pure sodium feldspar without waste glass), W5, W10 and W15. These mixes are referenced C0 (without waste glass), C3 (with 3% waste glass), C5 (with 5% waste glass), C7 (with 7% waste glass).

Raw materials	C0	C3	C5	C7
Clays	40	40	40	40
Kaolinitic sands	10	10	10	10
W0	50	-	-	-
W5	-	50	-	-
W10	-	-	50	-
W15	-	-	-	50

Table IV – *References and composition (wt%) of the ceramic mixes.*

To develop high strength ceramics, three alumina powders were used:

- Amorphous Alumina, gibbsite $Al(OH)_3$ - referenced AA
- Alumina Platelets, α-alumina - referenced AP
- Alumina Spheres, α-alumina - referenced AS

The morphological characteristics of the aluminas were observed by scanning electron microscope (SEM) and the images are showed in Fig. 1.

These materials were added in a fixed percentage, 5 wt%, in the best-performing ceramic mix chosen on the basis of the test results.

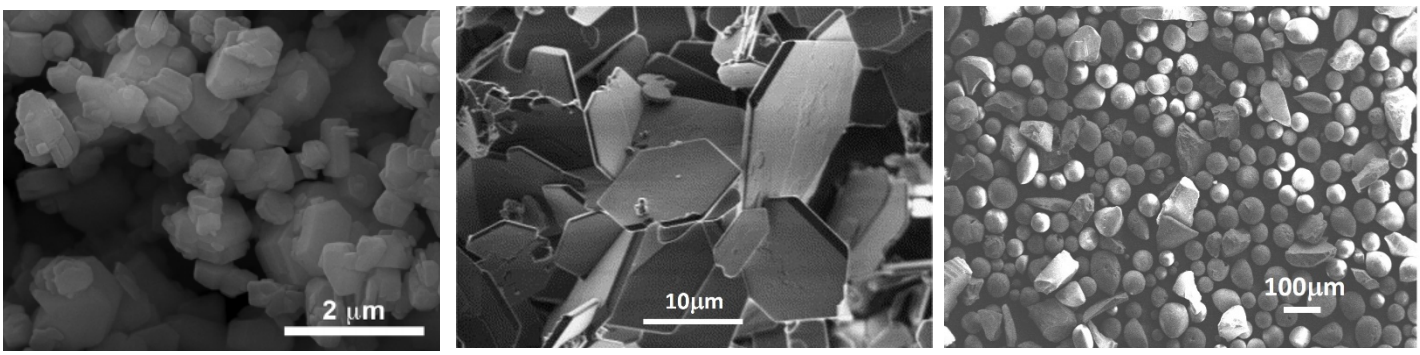

(a) (b) (c)

Figure 1 *– SEM-SE micrographs of alumina powders: amorphous alumina, AA (a); alumina platelets, AP (b) and alumina spheres, AS (c).*

All the mixes were prepared by wet milling the raw materials in a porcelain jar for 20 minutes and the dried powders, wetted with 7 wt% water, were uniaxially pressed at 30 MPa to obtain circular-shaped specimens (50 mm diameter and 7 mm height) or rectangular-shaped specimens (50x100 mm and 7 mm height).

Sintering behaviour was evaluated by firing the specimens at five different temperatures in a laboratory roller kiln and by measuring water absorption and linear shrinkage.

The quantitative mineralogical composition was determined of the fired specimens and the Crystalline Index was also calculated, according to the following equation:

$$Crystalline\ Index = \frac{\%\ new\ phases\ (*)}{\%\ residual\ phase + \%\ amorphous\ phase} x100$$

Mechanical performance was evaluated on the basis of flexural strength (by three-point bending test), Young's Modulus, Weibull modulus, Vickers hardness and fracture toughness.

3. RESULTS AND DISCUSSION

From Tab. V it is clear that the chemical composition of the ceramic mixes shows a decrease in alumina from C0 to C7 with the highest amount of waste glass, and an increase in CaO, MgO, Na_2O oxides and organic carbon (C) up to 0.20%.

By observing the graphic in Fig. 2, it is interesting to note that, maintaining constant the moisture of the specimens, the flexural strength of the dried samples seems to not vary from C0 to C5 but in C7 sample it increases a bit. It can be related to the higher amount of organic carbon that may improve the plasticity of the unfired samples.

	SiO_2	Al_2O_3	TiO_2	Fe_2O_3	CaO	MgO	Na_2O	K_2O	LOI	C	S
C0	70.3	18.3	0.5	0.7	1.0	0.3	3.3	1.8	3.9	0.05	0.01
C3	70.4	17.5	0.5	0.7	1.4	0.5	3.5	1.8	3.8	0.08	0.01
C5	70.6	16.7	0.5	0.7	1.8	0.6	3.6	1.8	3.8	0.11	0.01
C7	70.7	15.9	0.5	0.7	2.2	0.8	3.8	1.8	3.7	0.20	0.01

Table V *– Chemical composition of the ceramic mixes (wt%).*

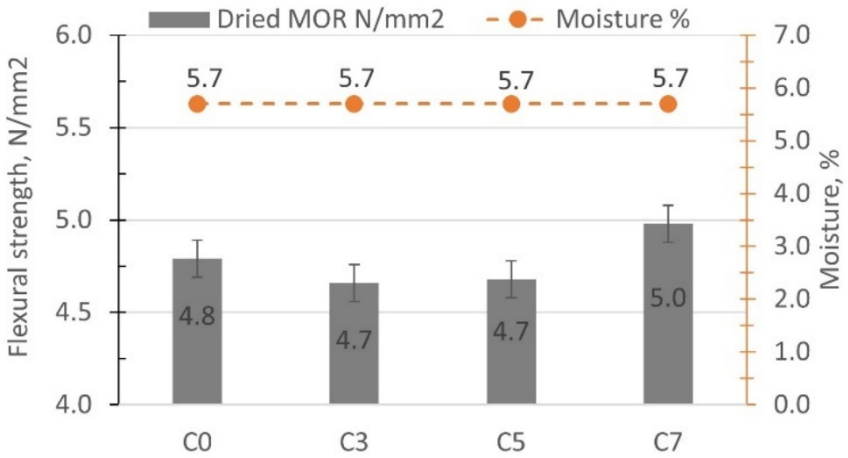

Figure 2 *– Characteristics of the unfired specimens in terms of flexural strength (histogram) and moisture content (orange points).*

The results of the firing behaviour are shown in Fig. 3 in terms of water absorption and linear shrinkage. From the C0 composition, without waste glass, to C7 with 7% waste glass, a significant reduction in the optimum sintering temperature is evident: from 1224°C to 1194°C. At the same time, a lower thermal stability is observed: the dotted black line shows an expansion after the optimal firing temperature, 1194°C, to 1214°C.

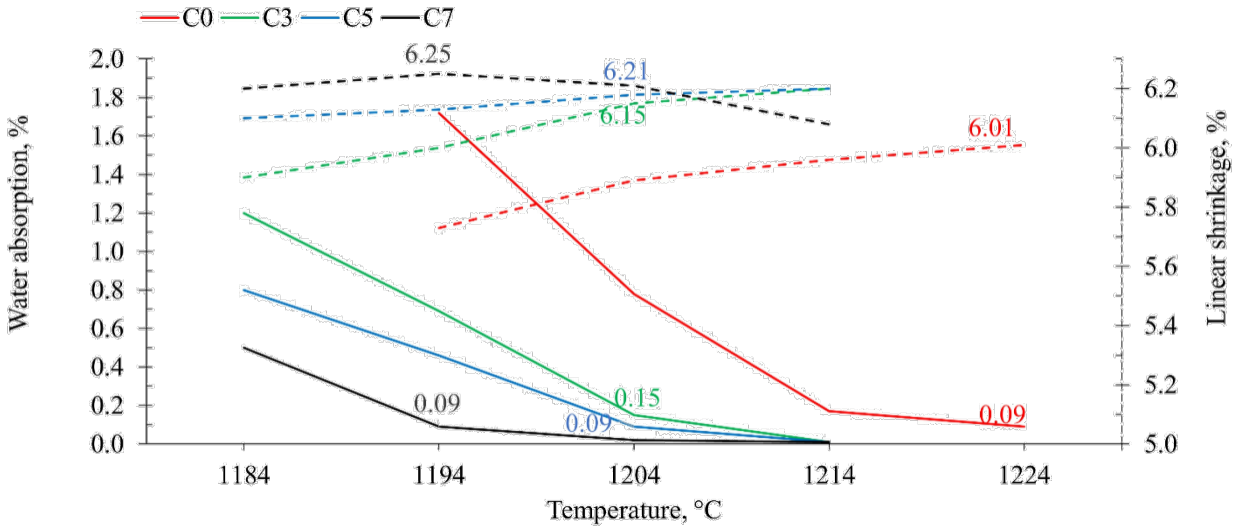

Figure 3 – *Firing behaviour of the ceramic mixes.*

Tab. VI shows the mineralogical composition of the samples. The new mixes, C3, C5, C7, even if they are fired at a lower temperature than that of reference C0 without waste glass, are characterized by a higher amount of newly formed crystals. In particular, sample C7 contains the highest amount of bytownite, a Ca-rich plagioclase.

The crystalline index, representing an index of the new crystals formed during firing, indicates the capability of the raw materials to interact synergically during firing. In C7 this index is the highest even if it is fired 30°C lower respect to the reference C0.

Also, the SEM micrographs indicate the presence of Ca-rich phases (Fig. 4).

Firing temperature	1224°C	1204°C	1204°C	1194°C	1204°C	1204°C	1204°C
	C0	**C3**	**C5**	**C7**	**C7AA**	**C7AP**	**C7AS**
Quartz	26	26	25	26	26	25	26
Mullite	4	4	2	1	9	2	1
Bytownite	-	2	6	11	10	12	11
Albite	6	5	5	7	5	5	7
K-feldspar	1	1	1	1	1	1	1
α-alumina	-	-	-	-	-	5	5
Amorphous phase	63	62	61	54	62	61	54
Tot.	100	100	100	100	100	100	100
Crystalline Index	**4**	**6**	**9**	**14**	**23**	**16**	**15**

Table VI *– Mineralogical composition of the ceramic mixes (wt%).*

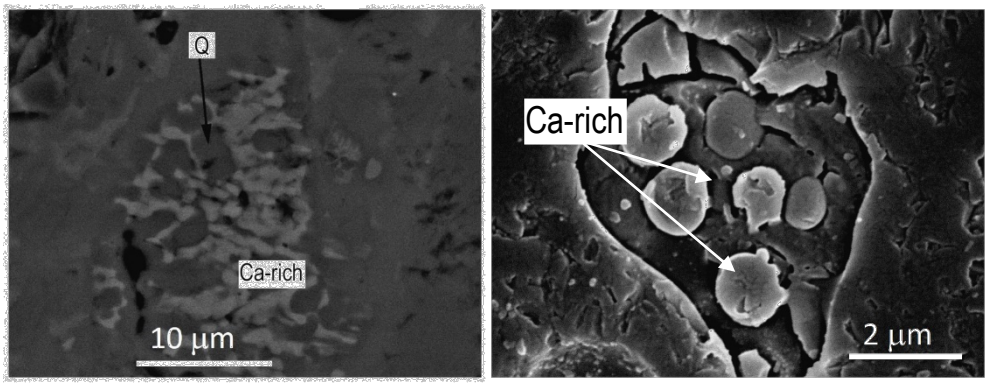

(a) (b)

Figure 4 *– SEM micrographs of sample C7 fired at 1194°C showing the presence of (a) calcium-rich phases (Ca-rich) within a quartz grain (Q) or (b) spheroidal particles.*

C7 composition was chosen to prepare new mixes with 5 wt% alumina additives: amorphous alumina (C7AA), α-alumina platelets (C7AP) and α-alumina spheres (C7AS).

As shown in Fig. 5, the firing behaviour of these new mixes shows an increase in the optimum firing temperature, from 1194°C to 1204°C (see the continuous lines). The dotted lines show a significant improvement of thermal stability with respect to C7, also at the highest temperature, 1224°C.

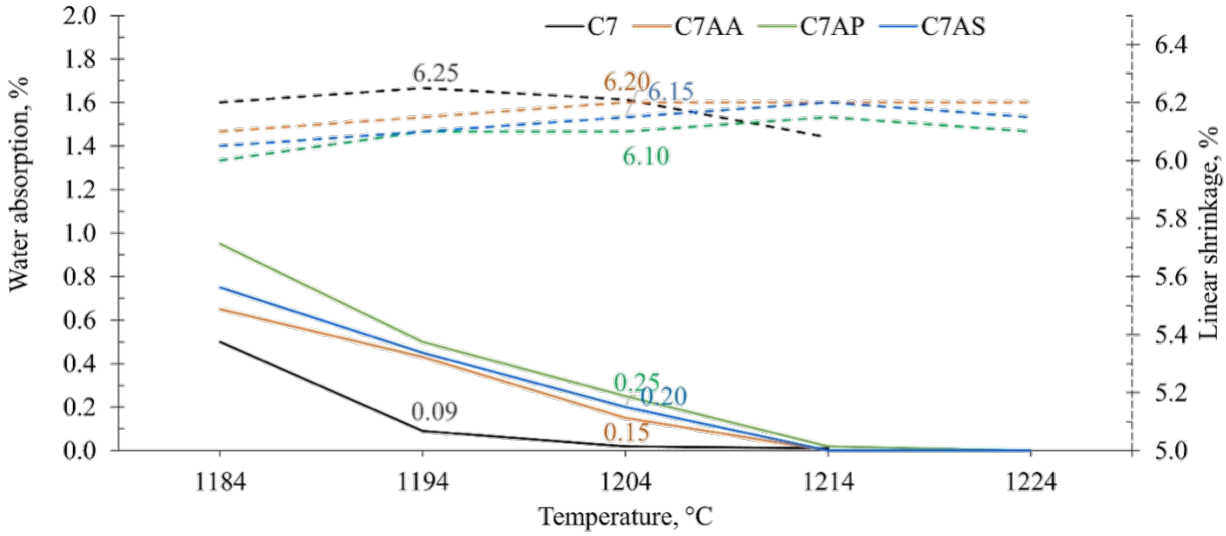

Figure 5 *– Firing behaviour of the ceramic-ceramic composites.*

The crystalline index (Tab. VI) is the highest in C7AA (23%), containing amorphous alumina that can react with raw materials, giving rise to the formation of mullite up to 9 wt% [2].

Corundum, α-alumina, was added (5 wt%) as platelets or spheres shapes in C7AP and C7AS, respectively, and it is not a new phase formed during sintering, thus it does not contribute to increasing the crystalline index. In these samples, the crystalline index remains similar to that of C7 but always higher than that of C0 (see Tab. VI).

SEM micrographs show the acicular-shaped mullite crystals in the C7AA etched surface (Fig. 6a), the α-alumina platelets embedded in the ceramic matrix in C7AP (see the yellow arrow in Fig. 6b) and the α-alumina spheres in C7AS (Fig. 6c).

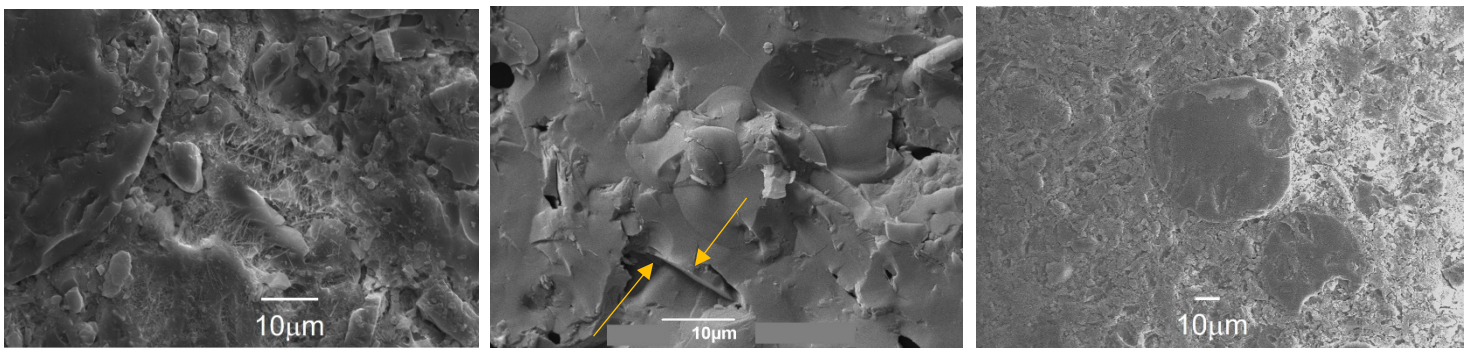

(a) (b) (c)

Figure 6 *– SEM micrographs of C7AA fired at 1204°C (a), C7AP fired at 1204°C (b) and C7AS fired at 1204°C (c).*

The mechanical performance (Tab. VII) of these new samples improved. In particular, flexural strength and Young's modulus increased significantly, especially in C7AP containing alumina platelets.

The Weibull modulus, a statistical parameter indicating the reliability of a material, improved in C7AA and C7AP, while in C7AS it was the lowest. It is important to evaluate the microstructure of these samples and the interfaces of α-alumina with the ceramic matrix (Fig. 7). A rather good adhesion was always observed in the C7AP sample (Fig. 7a). In the C7AS sample the adhesion of alumina spheres is not always good and sometimes partial detachments are observed (see the yellow arrow in the SEM micrograph of Fig. 7c). This decreases the reliability of the material significantly.

Vickers hardness improves slightly and fracture toughness improves in all the new mixes with alumina, especially in C7AP and C7AS with α-alumina platelets or spheres.

Firing temperature	1224°C	1194°C	1204°C	1204°C	1204°C
	C0	**C7**	**C7AA**	**C7AP**	**C7AS**
Flexural strength, MPa	53	58	62	85	73
Young's modulus, GPa	38	40	44	62	52
Weibull modulus, m	8	6	15	18	5
HV, GPa	nd	5.8	5.9	6.1	6.0
K_{IC} MPa.m$^{0.5}$	nd	1.6	1.8	2.1	2.0

Table VII *– Mechanical behaviour of the ceramic mixes.*

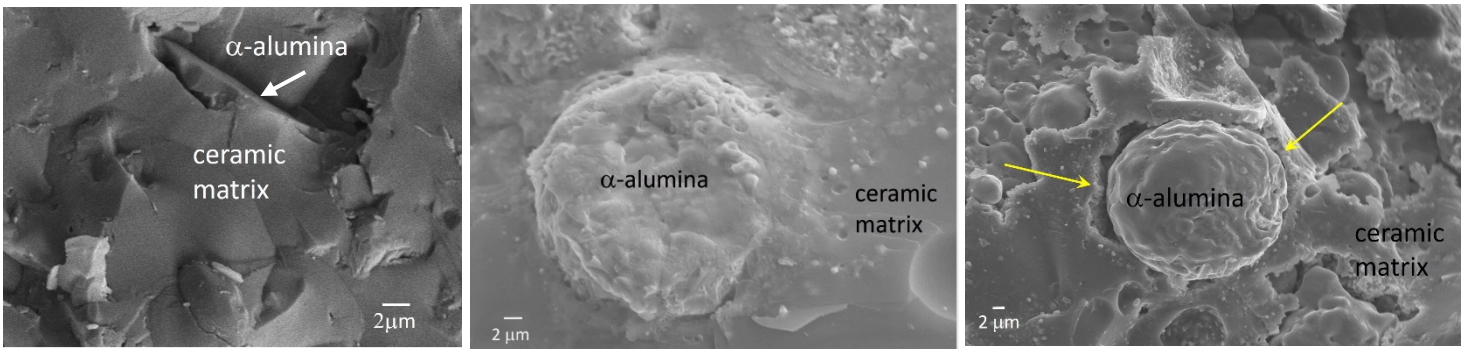

(a) (b) (c)

Figure 7 *– SEM micrographs of C7AP fired at 1204°C (a), C7AS fired at 1204°C (b) and C7AS fired at 1204°C with arrows indicating partial detachments (c).*

The reinforcing mechanisms are shown schematically for sample C7AS with alumina spheres, in terms of crack deflection and crack trapping [3].

In Fig. 8, the yellow dotted lines represent the Vickers indentation, and the red dotted curve represents the crack deflection.

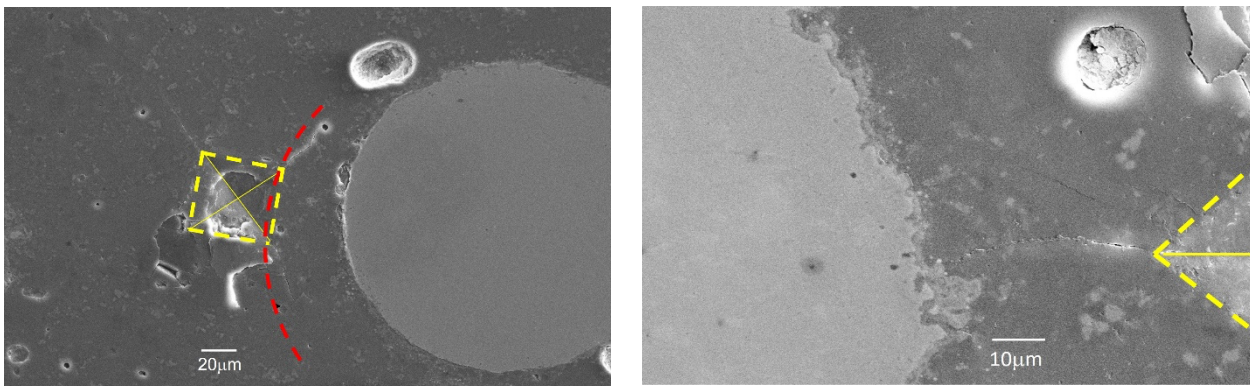

(a) (b)

Figure 8 *– SEM micrographs of C7AS fired at 1204°C showing crack deflection (a) and crack trapping (b). The yellow lines represent the Vickers indentation and the red line shows the deflection path.*

4. CONCLUSIONS

In conclusion, the new fluxes can significantly reduce the use of natural feldspars and the sintering temperature of ceramic tiles (at least 10°C lower). Moreover, the mechanical performance of ceramic-ceramic composites improves significantly, in particular the fracture toughness.

5. REFERENCES

[1] S. Maity, B.K. Sarkar, Development of high strength whiteware bodies, Journal of the European Ceramic Society, 16(10), 1996, 1083-1088.

[2] L.N.L. Santana, J. Gomes, R.R. Menezes, G.A. Neves, H.L. Lira, A.M. Segadaes, Microstructure development of clays upon heat treatment: Kinetics and equilibrium, Applied Clay Science, 135,2017, 325-332.

[3] C. Leonelli, F. Bondioli, P. Veronesi, M. Romagnoli, T. Manfredini, G.P. Pellacani, V. Cannillo, Enhancing the mechanical properties of porcelain stoneware tiles: a microstructural approach, Journal of the European Ceramic Society, 21(6), 2001, 785-793.